Results in Physics 36 (2022) 105470

Contents lists available at ScienceDirect

Results in Physics

journal homepage: www.elsevier.com/locate/rinp

Ultra-broadband nearly perfect absorbers based on graphene-coated lossy metallic nanostructures

Raha Khosravi [a], Yashar E. Monfared [b,*], Montasir Qasymeh [c]

[a] Rayleigh Solar Tech, Halifax, Nova Scotia, Canada
[b] Department of Chemistry, Dalhousie University, 6274 Coburg Road, Halifax, Nova Scotia, Canada
[c] Department of Electrical and Computer Engineering, Abu Dhabi University, United Arab Emirates

ARTICLE INFO

Keywords:
Lossy metals
Plasmonic metamaterial
Graphene plasmonics
Broadband absorber

ABSTRACT

In this paper, we present a new thin-film broadband nanostructured metamaterial absorber based on a graphene-coated plasmonic lossy metal–insulator–metal. Using the finite element method, we study the absorption properties of the proposed nanostructure and demonstrate the possibility of achieving an ultrabroad absorption spectrum by combining graphene and lossy metals. We demonstrate that graphene coating of the lossy metallic nano-disks improves the average absorption of the metamaterial by more than 10% while acts as a surface protection layer for the lossy metal films. Using the optimized design parameters and owing to the resonance coupling, a broad absorption from 400 nm to 2300 nm, particularly in the near-infrared region from 700 nm to 2000 nm, with a nearly flat absorption curve and an average absorption of 95.25% and a maximum absorption of 99.94% can be achieved. Other advantages of the proposed optical nano-absorber based on lossy metals instead of gold and silver include higher melting point (1668 °C compared to 1064 °C), the lower production cost of the metamaterial by using alternative materials, polarization insensitivity of the structure, and relative insensitivity to the radiation angle. In particular, the absorber maintains nearly an average of 90% absorptivity as the light incident angle reaches 30°. The proposed graphene-coated absorber demonstrates broader and stronger absorption, and much higher structural meting point compared to the previously reported thin-film based broadband absorbers, resulting in a viable platform for broadband applications with higher stability and durability.

Introduction

Broadband absorbers based on thin films, which can absorb incident electromagnetic radiations at frequency bands in visible, near infrared, infrared, and terahertz regions, attracted significant attention in the recent years [1–4]. These broadband absorbers can improve the efficiency and the overall performance of many leading-edge technologies including thermal emission tailoring [1], solar energy harvesting [2,3], and electromagnetic-based water desalination and purification [4]. Despite their potential, broadband absorbers based on thin films are difficult to realize in practical applications because of several design barriers [3,5]. For example, in thin-film-based absorbers, complete radiation absorption occurs only near resonances with limited bandwidths [5,6]. Additionally, high reflection at the films' interfaces with the surrounding environment, such as air or water, can prohibit absorbing incident radiation effectively [5,6].

Recently, metamaterials emerged as new potential platform to realize thin film based broadband absorbers thanks to their unique properties in controlling the electromagnetic radiations [5,6]. Metamaterials can be defined as periodic nanostructures which exhibit rare electromagnetic characteristics that cannot be found in conventional materials [6]. The absorption, scattering or extinction spectra of the metamaterials can be easily tuned by varying their design parameters, and as a result, shift their peak absorption or scattering to ultraviolet (UV), visible, infrared (IR) or even terahertz (THz) frequencies [7]. The combination of metamaterials and surface plasmon resonances (SPRs) can result in formation of plasmonic metamaterials. In plasmonic metamaterials, surface plasmons can be excited as a result of the interaction of the incident light with the metal–insulator interface between nanostructures and surrounding insulator layer [7]. One of the easiest configurations to fabricate plasmonic metamaterials is the metal–insulator–metal (MIM) configuration which is usually based on gold and silver nanofilms combined with an insulator material like SiO2 or Al_2O_3.

* Corresponding author.
E-mail addresses: raha@dal.ca (R. Khosravi), y.monfared@dal.ca (Y.E. Monfared), montasir.qasymeh@adu.ac.ae (M. Qasymeh).

https://doi.org/10.1016/j.rinp.2022.105470
Received 3 March 2022; Received in revised form 23 March 2022; Accepted 27 March 2022
Available online 29 March 2022

In recent years, various plasmonic metamaterial absorbers based on thin metal films have been studied and utilized as nearly-perfect absorbers from the IR to the visible and UV ranges. Some of these studies also demonstrate wavelength insensitivity to the angle of incidence of incoming electromagnetic wave and incident light polarization [6,8,9]. Most of the metamaterials are based on gold (Au) and silver (Ag) as plasmonic material in the resonator layer. Usually, these metamaterial absorbers are only efficient within a very narrow band due to their narrow-band resonance property, which limits the application of these metamaterial absorbers for many practical scenarios. There are a few main strategies to achieve a large absorption bandwidth in thin-film plasmonic metamaterial absorbers. A common technique is to combine spectrally adjacent resonances which can be done by excitation of several multi-sized resonators at the same time [10]. While this technique may lead to broader resonances, the number of the resonators one can use in the metamaterial structure is restricted because of the neighboring resonances competition [6,10]. Also, the absorption performance is sensitive to several structural design parameters, which can be hard to maintain in the fabrication process [10]. As such, scientists look for alternative solutions to broaden the resonance while maintaining simple metamaterial designs.

One of the best possible solutions is to utilize a lossy plasmonic material instead of mainstream plasmonic materials (Au and Ag) as the resonator material [2,6]. For example, titanium (Ti), nickel (Ni), tungsten (W) and magnesium (Mn) as lossy plasmonic materials can exhibit broader resonances compared to Au and Ag. Furthermore, they are far more cost-effective than their noble metal counterparts [6] which can help in scaling the production of the broadband absorbers. The absorption range of the metamaterial absorber can be further broadened and enhanced by using graphene coating layers in the plasmonic metamaterial structure. Graphene can not only offer improved absorption properties, but also can act as a surface protection coating layer for the plasmonic nanofilms [11–13]. Here, we propose a broadband thin film metamaterial absorber based on a graphene-coated plasmonic metamaterial with MIM configuration via four different lossy materials (Ni, Ti, W, and Mn) for the resonators. Our proposed plasmonic metamaterial can offer a solution to the limitation of the conventional broadband thin-film absorbers by increasing the absorption efficiency and bandwidth, yet with simple MIM configuration. These combined advantages pave the way for achieving low-cost and ultra-broadband electromagnetic absorbers with potential applications in disruptive technologies like solar energy harvesting, thermal energy conversion, and surface disinfection.

Design, materials, and methods

The schematic of our thin-film graphene-coated metamaterial broadband absorber with lossy metals (Ni, Ti, Mn, and W), and the geometry of the unit cell of the plasmonic metamaterial are illustrated in Fig. 1a and 1b, respectively. Here, a broadband light source is considered irradiating normally to the nanodisks surface. The broadband absorber consists of periodic nano-disk array made from a lossy metal, and an insulator layer metal film which is separated from the nano-disks (resonating layer) by a silicon dioxide (SiO_2) dielectric layer. In conventional MIM configurations, Au is usually used as the ground material. In this work, the ground and the resonating layers (i.e., nano-disks) are considered of the same metal. The main reason for not using Au as the ground layer is its low melting point and higher production costs of Au [14]. For instance, conventional metamaterial and nanomaterial absorbers that utilize noble metals (Au and Ag) suffer from structural damages caused by high temperatures resulting from strong plasmonic photo-thermal effect [14]. Using Ni, Ti, Mn or W as the bottom layer will provide stable metamaterial even under higher temperatures due to higher melting point of these metals compared to Au and Ag [15].

To this end, and by conducting intensive numerical investigations to optimize the proposed metamaterial configuration, the topmost nano-disks which are periodically distributed in x- and y-directions are considered with a gap size of g = 250 nm. Furthermore, in the unit cells the diameter and the thickness of the nano-disks are set to be d = 390 nm and t_d = 35 nm, respectively.

Here a single graphene layer ($t_{graphene} = \Delta = 0.34$ nm) is used to coat the plasmonic nano-disks which can offer advantages like improved surface stability of the lossy metals (no oxidation), and improve absorption bandwidth and strength of the absorber (particularly in the visible range). The SiO_2 insulator layer thickness is optimized to be $t_{si} =$ 30 nm, and the ground lossy metal film has a thickness of $t_g = 120$ nm, which can block almost all transmission in visible and near IR frequencies. In the unit cell, the lossy metals and SiO_2 films have equal width and length ($W = L = 600$ nm). In this paper, we use three dimensional full-wave simulations have been performed via finite element method (FEM) applied with COMSOL Multiphysics software to verify the performance of the graphene-coated broadband absorber. In our FEM model, we model the structure by designing a single unit cell and applying periodic boundary conditions on the vertical sides of the cell which results in electromagnetic response for the whole periodic structure. In the model and for initial simulations, the incident wave is assumed to be a plane wave propagating normal to the surface and then we eventually examined various incident angles. In the metal-SiO_2-metal-graphene configurations, the complex index of refraction of Ni, Ti, Mn, and W are obtained from the available experimental data [16,17]. The real and imaginary parts of dielectric functions of Ni, Ti, Mn, and W are plotted in Fig. 2a, 2b, 2c, and 2d, respectively, for reference.

In our model, we consider the effect of the material dispersion of SiO_2 to improve the accuracy of the simulations. The refractive index of SiO_2 as a function of the incident light wavelength is given by the following Sellmeier's equation [7],

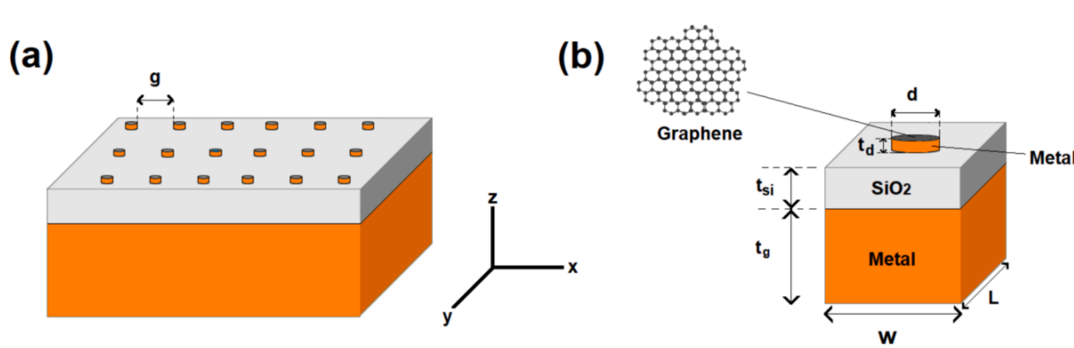

Fig. 1. (a) Schematic of our graphene-coated thin-film metamaterial broadband absorber with gap size *g* between nano-disks, and (b) The plasmonic metamaterial unit cell with nano-disk diameter *d*, width of the unit cell *W*, length of the unit cell *L*, thickness of lossy metal disks t_d, thickness of SiO_2 layer t_{si} and thickness of ground layer lossy metal t_g.

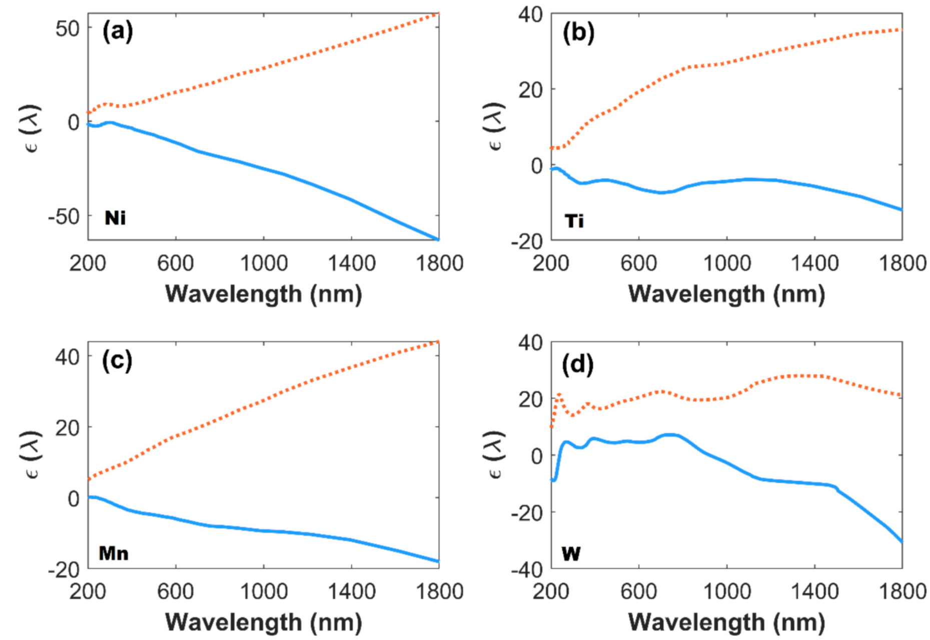

Fig. 2. Real part (solid blue lines) and imaginary part (dashed orange lines) of dielectric function of lossy metals: (a) nickel, (b) titanium, (c) manganese, and (d) tungsten, as a function of wavelength. (For interpretation of the references to colour in this figure legend, the reader is referred to the web version of this article.)

$$n_{SiO2}^2 = 1 + \frac{0.6961663\lambda^2}{\lambda^2 - 0.0684043^2} + \frac{0.4079426\lambda^2}{\lambda^2 - 0.1162414^2} + \frac{0.8974794\lambda^2}{\lambda^2 - 9.896161^2} \tag{1}$$

where λ is the incident light wavelength. The single graphene coating film is modeled as an ultrathin layer with thickness Δ and effective bulk permittivity ε_{eff}. The effective permittivity of graphene is given by [18],

$$\varepsilon_{\rm eff} = \varepsilon_0 - \frac{Im(\sigma_s)}{\omega\Delta} + i\frac{Re(\sigma_s)}{\omega\Delta} \tag{2}$$

where $\omega = 2\pi f$, and ε_0 is the free space permittivity, Δ is the thickness of the graphene layer (0.34 nm) and σ_s is the graphene conductivity, given by [18],

$$\sigma_s = \frac{iq^2}{4\pi\hbar} ln\left(\frac{2\mu_c - (f + i\tau^{-1})\hbar}{2\mu_c + (f + i\tau^{-1})\hbar}\right) + \frac{iq^2 K_B T}{\pi\hbar^2 (f + i\tau^{-1})}\left(\frac{\mu_c}{K_B T} + 2ln\left(e^{-\frac{\mu_c}{K_B T}} + 1\right)\right), \tag{3}$$

The first term in Eq. (3) represents the interband conductivity of graphene while the second term demonstrate the intraband conductivity of graphene. In Eq. (3), q represents the electron charge, ħ is the reduced plank's constant, τ is the scattering relaxation time, K_B is the Boltzman constant, T represents temperature which is considered to be 300 K at this case, f expresses frequency, and finally μ_c is the graphene chemical potential which here considered to be 0.3 eV. In our model, the medium surrounding the broadband absorber is considered to be the air with unit refractive index in the simulations.

Results and discussions

Broadband absorption performance

We calculate the absorption spectra of the proposed plasmonic absorber via a FEM model by obtaining transmission and reflection spectra of the structure. We first analyze the light absorption properties of the plasmonic nanostructure shown in Fig. 1a using a lossy metal-SiO2-lossy metal without graphene as a coating layer. As expected, the power transmission in visible and near IR regions were nearly zero through the metamaterial because of the relatively thick ground layer (120 nm) for all lossy metals. As such, we can obtain absorption spectra of the nanostructures in the visible and IR region by simply measuring the reflection spectra. Here however, we consider the weak transmission in visible and near IR regions for more accurate results and calculated absorbance (A) using both reflectance (R) and transmittance (T) as, A = 1 – R – T.

The calculated absorption spectra of metal-SiO_2-metal structure with various metals are presented in Fig. 3a. It is clear that the metamaterials with lossy metals have significantly broader resonances (absorption spectra) in the visible and infrared (IR) regions between 600 nm and 2200 nm. Among all considered lossy metals, Ti and Mn possess the broadest absorption spectral range as demonstrated in Fig. 3b where the average absorption of all considered metals can be compared to each other. In particular, Ti-SiO2-Ti metamaterial exhibit a significantly broad absorption spectrum with two distinguished peaks at $R_1 = 855$ nm and $R_2 = 1342$ nm. The first resonance (R_1) has a smaller full-width at half maximum (FWHM) while R_2 is significantly broader and has a larger absorption magnitude compared to the first peak.

To examine the role of graphene coating on the absorption properties of structure, we compare the absorption of the Ti-SiO_2-Ti metamaterial with and without graphene coating in Fig. 4a. Based on the results of Fig. 4, graphene coating of Ti nano-disks improves the absorption magnitude and therefore broadness of the absorption of the nanostructure in visible and near IR regions. Another difference we observe in the simulations is that the absorption peak for both resonances redshift by introducing graphene coating (R_1 from 855 to 881 nm and R_2 from 1342 to 1362 nm). In addition, the numerical simulations demonstrate that graphene-coated nanostructure have significantly higher average absorption magnitude in the visible and near IR region compared to nanostructure without graphene coating as demonstrated in Fig. 4b. The improvement in the absorption broadness and magnitude is probably due to different optical losses of graphene-Ti hybrid nano-disks compared to Ti nano-disks without graphene coating.

Physical mechanism of resonances

In this section, we explore the physical mechanism of resonances in the proposed nanostructure which can help us to fully understand the absorption properties of the device. As a result, the electric and magnetic fields around the absorption peak positions close to resonances (at 881 nm resonance and 1362 nm resonance) have been analyzed in detail.

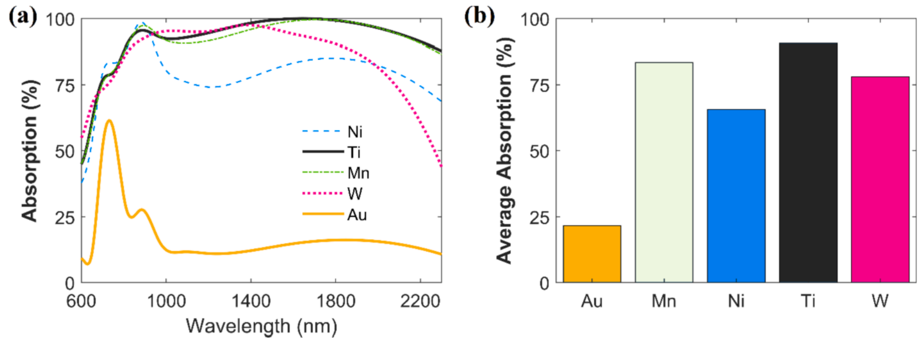

Fig. 3. (a) Broadband absorption of lossy metal-SiO_2-lossy metal nanostructure with various lossy metals and optimized design parameters described in section 2 compared to Au-SiO_2-Au structure. (b) Comparison between average absorption of various lossy metals and Au between 600 and 2200 nm wavelength range.

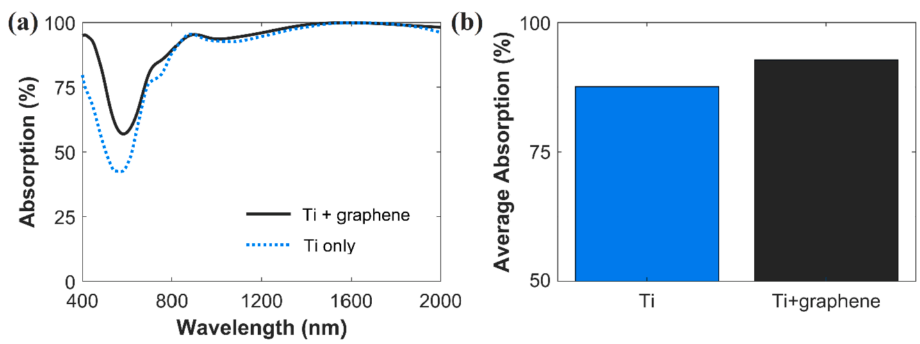

Fig. 4. (a) Normalized absorption of the proposed Ti-SiO_2-Ti-graphene metamaterial absorber with and without graphene coating of Ti nano-disks between 400 nm and 2000 nm. (b) Comparison between average absorption of the metamaterial absorbers with and without graphene coating of Ti nano-disks.

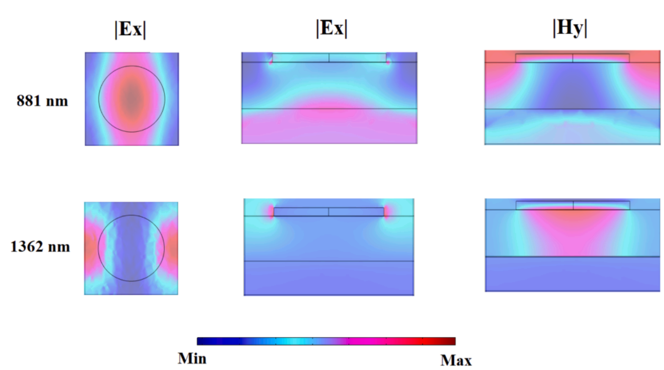

Fig. 5. The distributions of electric |Ex| and magnetic |Hy| fields in the proposed nanostructured graphene-coated broadband absorber around two resonances (R_1 and R_2) in the x-y (first column), and y-z (second and third columns) planes.

Fig. 5 illustrates the normalized electric (|Ex|) and magnetic (|Hy|) field distributions close to the nanostructure resonances (around R_1 and R_2) in x-y and x-z planes. These unique resonances can be explained as electric dipole resonances excited on the graphene-coated nano-disks or between the disks.

The first resonance around R_1 is a hybrid plasmonic mode which composed of surface plasmon polariton (SPP) resonance between the ground metal nanofilm and the silica nanofilm, and also localized surface plasmon resonance (LSPR) on the edges of the graphene-coated nano-disks. The coexistence of the SPP and LSPR resonances can be clearly seen from the dual magnetic field enhancement in both the adjacent graphene-coated nano-disks and the silica layers. The resonance mode at R_2 is however a fundamental LSPR mode where the magnetic field is mainly trapped within the gap between the topmost graphene-coated nano-disks and the ground layer lossy metal nanofilm while there is no significant coupling between the graphene-coated nano-disks.

It should be noted that most of the absorption in near IR region is coming from the graphene-coated lossy metal nano-disks as the absorption of lossy metal ground layer is weak for λ greater than 900 nm which indicates that the lossy metal ground layer mainly operates as a mirror to reflect the incoming electromagnetic waves in these frequencies. In the visible wavelengths (and a small region inside near IR) where $\lambda < 900$ nm, the ground lossy layer can directly dissipate some of the light which can leads to the generated hybrid SPP-LSPR resonance around R_1.

The effects of the design parameters and incident angle on absorption properties

The design parameters selected in this paper, including the previous simulations, are obtained by conducting numerical investigations to achieve the broadest possible absorption spectra. In this section, we study the design parameters' role on the absorption spectra of the proposed plasmonic nanostructure. The considered design parameters are chosen large or small relative to the optimized values in this paper to clearly show the variations of absorption spectra based on using different design parameters. We illustrate the results of our numerical investigations in Fig. 6. First, we study the role of the thickness of the graphene-coated nano-disks on the absorption spectra in the proposed nanostructure, as illustrated in Fig. 6a. By increasing the thickness of graphene-coated nano-disks from 25 nm to 35 nm, the absorption peak close to R_2, redshifts from 1316 nm to 1547 nm. The absorption peak around R_1 also redshifts by increasing the nano-disks thickness with much smaller values than R_2. Next, the role of the thickness of silica insulator film is studied in Fig. 6b. By increasing the thickness of the silica layer from 150 nm to 170 nm, the absorption maximum

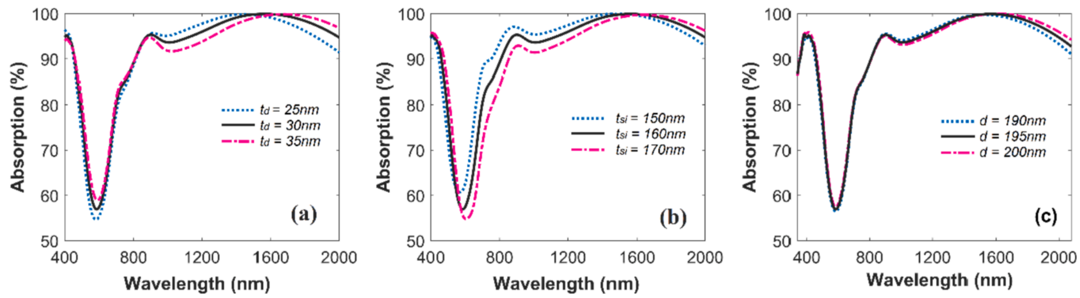

Fig. 6. The effect of the design parameters on the absorption spectra of the proposed Ti-Si-Ti-graphene where (a) thickness of graphene-coated nano-disks t_d varies between 25 nm and 35 nm, (b) thickness of silica insulator layer t_{si} varies between 150 nm and 170 nm, and (c) graphene-coated nano-disks diameter d changes between 190 nm and 200 nm.

wavelengths around R_1 and R_2 shift towards the longer wavelengths. However, the magnitude of the absorption peaks reduces slightly. Finally, the effect of graphene-coated nano-disk diameters on the absorption spectra of the proposed nanostructure is studied in detail in Fig. 6c. Interestingly, slight variation in the diameter of the nano-disks does not significantly affect the location, intensity, or broadness of the resonances in our structure. It should be noted that according to these results, small changes in design parameters like thickness of films (±5 nm) which can be happen because of the fabrication-induced imperfections cannot change the absorption spectra of our proposed broadband absorber by much.

In previous sections, we studied a situation when the incident light is normal to the surface of the metamaterial absorber. As the incident angle in industrial applications can be oblique [19], we investigate the absorption spectra of the proposed metamaterial for non-normal incidence. To this end, we perform full-wave simulations with varying incident angles and demonstrate the results in a contour plot. As seen in Fig. 7, the absorption spectrum is nearly robust for a relatively wide range of incident angles. Our numerical studies reveal that the ultra-broadband absorption spectra can be achieved when the angle of incidence is below 30°. It should be noted that the absorption still remains around 90% even when the incident angle reaches 30°. Therefore, our proposed broadband absorber is relatively insensitive to small variations in the design parameters (fabrication-induced imperfections) and angle of incidence which makes it more attractive for various real-world applications.

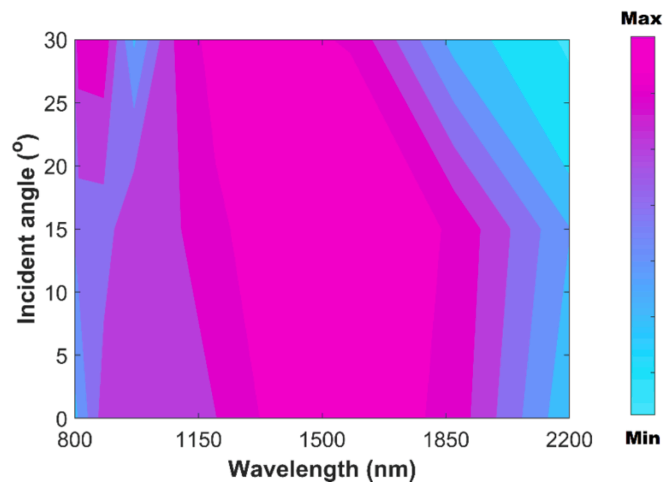

Fig. 7. The contour plot of the absorption spectrum of the proposed Ti-Si-Ti-graphene nanostructure depending on various incident angles between 0 and 30°.

Conclusions

In summary, different broadband plasmonic metamaterial absorbers in metal–insulator-metal structure using various lossy metals with high melting points including titanium (Ti), nickel (Ni), tungsten (W) and magnesium (Mn) have been studied in detail. We demonstrated that the combination of Ti as the lossy material in nano-disks, and graphene as a coating material can result in extremely broad and efficient light absorption in the visible and near-infrared regions. We particularly showed that using graphene as a coating layer for lossy-metal nano-disks improves the average absorption of the plasmonic nanostructure by more than 10% while offer surface protection and stability as a coating layer for the lossy metals. Using the optimized design parameters, a broad absorption spectrum ranging from 400 nm to 2200 nm (with a flat absorption with more than 95% average absorption from 700 nm to 2000 nm) can be achieved. We also demonstrated that the platform is almost insensitive to variations in the incident angle, or small fabrication-induced imperfections. The findings of this work hold promising potential to develop efficient and practical broadband absorbers in various industries, including solar absorbers, enabling different applications.

Funding

This research is supported by the ASPIRE Award for Research Excellence under the Advanced Technology Research Council (ASPIRE) (AARE19-062) 2019.

Declaration of Competing Interest

The authors declare that they have no known competing financial interests or personal relationships that could have appeared to influence the work reported in this paper.

References

[1] Ji T, Li H, Wang W, Wu X, Cui Y, Jia Z, et al. Metal-island-film-based plasmonic triple-layer absorber. J Opt Soc Am B 2018;35(6):1469. https://doi.org/10.1364/JOSAB.35.001469.
[2] Sun Z, Huang F, Fu Y. MoS2-based broadband and highly efficient solar absorbers. Appl Opt 2020;59(22):6671. https://doi.org/10.1364/AO.399772.
[3] Zeng Li, Zhang X, Ye H, Dong H, Zhang H. Design of ultra-broadband absorption enhancement in plasmonic absorber by interaction resonance of multi-plasmon modes and Fabry-Perot mode. Opt Express 2021;29(18):29228. https://doi.org/10.1364/OE.440172.
[4] Sreedhar A, Noh JS. Advancements in Solar Desalination of Seawater by Various Ti3C2 MXene Based Morphologies for Freshwater Generation: A Review. Catalysts 2021;11:1435.
[5] Pu M, Feng Q, Wang M, Hu C, Huang C, Ma X, et al. Ultrathin broadband nearly perfect absorber with symmetrical coherent illumination. Opt Express 2012;20(3):2246. https://doi.org/10.1364/OE.20.002246.
[6] Ding F, Dai J, Chen Y, Zhu J, Jin Y, Bozhevolnyi SI. Broadband near-infrared metamaterial absorbers utilizing highly lossy metals. Sci Rep 2016;6:39445.
[7] Monfared YE, Qasymeh M. Graphene-Assisted Infrared Plasmonic Metamaterial Absorber for Gas Detection. Res Phys 2021;23:103986.

[8] Zhong YK, Lai Y-C, Tu M-H, Chen B-R, Fu SM, Yu P, et al. Omnidirectional, polarization-independent, ultra-broadband metamaterial perfect absorber using field-penetration and reflected-wave-cancellation. Opt Express 2016;24(10):A832. https://doi.org/10.1364/OE.24.00A832.
[9] He Y, Deng H, Jiao X, He S, Gao J, Yang X. Infrared perfect absorber based on nanowire metamaterial cavities. Opt Lett 2013;38(7):1179. https://doi.org/10.1364/OL.38.001179.
[10] Qin Z, Shi X, Yang F, Hou E, Meng D, Sun C, et al. Multi-mode plasmonic resonance broadband LWIR metamaterial absorber based on lossy metal ring. Opt Express 2022;30(1):473. https://doi.org/10.1364/OE.446655.
[11] Esfahani Monfared Y, Qasymeh M. Plasmonic Biosensor for Low-Index Liquid Analyte Detection using Graphene-Assisted Photonic Crystal Fiber. Plasmonics 2021;16(3):881–9.
[12] Hayati Raad S, Atlasbaf Z, Monti A, Toscano A, Bilotti F. On the surface impedance modeling of metasurfaces composed of graphene-coated spherical nanoparticles. J Opt Soc Am B 2022;39(3):917. https://doi.org/10.1364/JOSAB.448936.
[13] Huang Q, Zhong L, Dong J, Xu Ou, Zheng Z, Huang T, et al. All-optical light manipulation based on graphene-embedded side-polished fiber. Opt Lett 2022;47(6):1478. https://doi.org/10.1364/OL.452612.
[14] Chen Z, Fan H, Li J, Tie S, Lan S. Photothermal therapy of single cancer cells mediated by naturally created gold nanorod clusters. Opt Express 2017;25(13):15093. https://doi.org/10.1364/OE.25.015093.
[15] Takahara W. Melting points and chemical bonding properties of 3d transition metal elements. IOP Conf Ser: Mater Sci Eng 2014;61:012029. https://doi.org/10.1088/1757-899X/61/1/012029.
[16] Johnson P, Christy R. "Optical constants of transition metals: Ti, V, Cr, Mn, Fe Co, Ni, and Pd. Phys Rev B 1974;9(12):5056–70.
[17] Ordal MA, Bell RJ, Alexander RW, Newquist LA, Querry MR. Optical properties of Al, Fe, Ti, Ta, W, and Mo at submillimeter wavelengths. Appl Opt 1988;27(6):1203. https://doi.org/10.1364/AO.27.001203.
[18] Qasymeh M, Eleuch H. Quantum microwave-to-optical conversion in electrically driven multilayer graphene. Opt Express 2019;27(5):5945. https://doi.org/10.1364/OE.27.005945.
[19] Gao FW, Sui C, Zhou S, Fu SF, Wang X, Song YL, et al. Actively tunable terahertz metasurface absorber due to surface phonon polaritons. J Opt Soc Am B 2022;39(4):1195. https://doi.org/10.1364/JOSAB.443778.